Hydrol. Earth Syst. Sci. Discuss., https://doi.org/10.5194/hess-2017-441
Manuscript under review for journal Hydrol. Earth Syst. Sci.
Discussion started: 25 August 2017

Hydrology and Earth System Sciences
Open Access
Discussions

Modeling water balance using the Budyko framework over variable timescales under diverse climates

Chuanhao Wu[1], Pat J.-F. Yeh[2], Kai Xu[1], Bill X. Hu[1*], Guoru Huang[3,4], and Peng Wang[1,5]

[1]Institute of Groundwater and Earth Sciences, Jinan University, Guangzhou 510632, China.
[2] Department of Civil and Environmental Engineering, National University of Singapore, Singapore.
[3]School of Civil Engineering and Transportation, South China University of Technology, Guangzhou 510640, China.
[4] State Key Laboratory of Subtropical Building Science, South China University of Technology, Guangzhou 510640, China.
[5] Chongqing Key Laboratory of Karst Environment, Chongqing 400715, China.

Correspondence to: Bill X. Hu (bill.x.hu@gmail.com)

Abstract

Understanding the effects of climate and catchment characteristics on overall water balance at different temporal scales remains a challenging task due to the large spatial heterogeneity and temporal variability. Based on a long-term (1960–2008) land surface hydrologic dataset over China, this study presented a systematic examination of the applicability of the Budyko model (BM) under various climatic conditions at long-term mean annual, annual, seasonal and monthly temporal scales. The roles of water storage change (*WSC*, *dS*/*dt*) in water balance modeling and the dominant climate control factors on modeling errors of BM are investigated. The results indicate that BM performs well at mean annual scale and the performance in arid climates is better than humid climates. At other smaller timescales, BM is generally accurate in arid climates, but fails to capture dominant controls on water balance in humid climates due to the effects of *WSC* not included in BM. The accuracy of BM can be ranked from high to low as: dry seasonal, annual, monthly, and wet seasonal timescales. When *WSC* is incorporated into BM by replacing precipitation (*P*) with effective precipitation (i.e., *P* minus *WSC*), significant improvements are found in arid climates, but to a lesser extent in humid climates. The ratio of the standard deviation of *WSC* to that of evapotranspiration (*E*), which increases from arid to humid climates, is found to be the key indicator of the BM simulation errors due to the omission of the effect of *WSC*. The modeling errors of BM are positively correlated with the temporal variability of *WSC* and hence larger in humid climates, and also found to be proportional to the ratio of potential evapotranspiration (*PET*) to *E*. More sophisticated models than the BM which explicitly incorporate the effect of *WSC* are required to improve water balance modeling in humid climates particularly at all the annual, seasonal, and monthly timescales.

Key words: water balance; Budyko framework; evapotranspiration; water storage change; China

1 Introduction

Precipitation (*P*) partitioning into evapotranspiration (*E*), runoff (*R*) and soil water storage is controlled by climate and catchment characteristics, such as soil, topography, and vegetation (Zhang et al., 2008). Quantifying the effects of climate and catchment characteristics on water balance is a major scientific challenge for hydrologists. Budyko (1958) postulated that the first-order control on the partitioning of *P* is the balance between available water (*P*) and energy (represented by potential evapotranspiration, *PET*). The empirical relationship proposed, widely known as the Budyko's curve, has shown good agreement with long-term water balance data for numerous watersheds globally (Budyko, 1974). Based on the Budyko hypothesis, various functional forms associated with the relation between the evaporation ratio (*E*/*P*) and climate aridity index (*PET*/*P*) have been developed for quantifying long-term water balance (Pike, 1964; Fu, 1981; Choudhury, 1999; Zhang et al., 2001, 2004; Porporato et al., 2004; Yang et al., 2008; Gerrits et al., 2009). The parameters of the analytically derived Budyko-type equations (e.g., Fu, 1981; Zhang et al., 2004; Yang et al., 2008) well account for the effects of rainfall seasonality and soil water storage capacity (Milly, 1994a, 1994b; Potter et al., 2005; Hickel and Zhang, 2006; Yokoo et al., 2008; Gerrits et al., 2009; Feng et al., 2012) and vegetation dynamics (Zhang et al., 2001; Donohue et al., 2007; Oudin et al., 2008; Yang et al., 2009; Peel et al., 2010; Li et al., 2013; Zhang et al., 2016) on the long-term mean water-energy balance. The Budyko framework has been considered as a useful tool to investigate the interaction between climate, the hydrologic cycle, and catchment characteristics under the steady state at the catchment scale (Donohue et al., 2007, 2010, 2011; Yang et al., 2009; Roderick and Farquhar, 2011; Wang and Hejazi, 2011; Yang and Yang, 2011; Li et al., 2013; Zhang et al., 2016).

Recently numerous research efforts have been directed to extend the applicability of the original Budyko framework to smaller temporal scales than the long-term average, such as annual (Koster and Suarez, 1999; Sankarasubramanian and Vogel, 2002; Zhang et al., 2008; Yang et al., 2007, 2009; Potter and Zhang, 2009; Cheng et al., 2011; Tekleab et al., 2011; Carmona et al., 2014; Yu et al., 2013), seasonal (Chen et al., 2013), monthly (Zhang et al., 2008; Tekleab et al., 2011; Du et al., 2016), and daily (Zhang et al., 2008) timescales. For example, Koster and Suarez (1999) proposed an analytical

framework based on the Budyko equation to quantify the interannual variability of *E*, and compared the theoretical framework with the global climate model simulations. Zhang et al. (2008) extended the Budyko framework to predict water balance at the mean annual, annual, monthly, and daily timescales in Australia. The results indicated that the models perform well in most catchments in Australia at the mean annual and annual timescales, but more complicated models are required at the shorter timescales primarily due to the importance of water storage change (*WSC*, *dS*/*dt*) at these smaller timescales. Yang et al. (2009) incorporated the impact of vegetation coverage into the Budyko framework to improve parameter estimation in the coupled water-energy balance equation. Chen et al. (2013) extended the Budyko framework to the seasonal timescale and also developed a model for incorporating interannual variability of *E* and *WSC*. The *WSC* has been found to be a significant component on water balance variability at annual or smaller timescales in many regions around the world (Eltahir and Yeh, 1999; Yeh and Famiglietti, 2008; Yokoo et al., 2008; Istanbulluoglu et al., 2012; Wang and Alimohammadi, 2012; Wang, 2012; Chen et al., 2013; Du et al., 2016). Wu et al. (2017) investigated the effects of climate and *WSC* on the temporal variability of *E* over China. They found that the effect of *WSC* in accommodating climatic fluctuations is larger at monthly timescale than at annual timescale, and even becomes the dominant controlling factor on the temporal variability of *E* in some extremely arid regions. Therefore, when applying to smaller timescales, the Budyko framework should be extended to incorporate the effect of *WSC* (Zhang et al., 2008; Zeng and Cai, 2015). Wang (2012) suggested that the effective precipitation (i.e., *P* minus *WSC*) can be used in Budyko's framework to account for the storage change and satisfy the water balance under the non-steady-state condition.

Although advances have been made in water balance simulations over variable timescales within the Budyko framework, our knowledge about the effects of climate and catchment characteristics on the water balance is still limited due to its spatial heterogeneity and temporal variability. The research question asked in this study is whether the Budyko framework is applicable for water balance modeling at smaller timescales when *WSC* becomes increasingly significant, and under various hydroclimate conditions particularly for the extremely humid or arid climates. On the basis of a long-term (1960–2008) gridded land surface dataset over China, the objectives here are: (1) to test the Budyko framework under various climatic conditions over four different timescales (mean annual, annual, seasonal, and monthly) at both the basin and the grid scales;

Hydrol. Earth Syst. Sci. Discuss., https://doi.org/10.5194/hess-2017-441
Manuscript under review for journal Hydrol. Earth Syst. Sci.
Discussion started: 25 August 2017

(2) to investigate the role of *WSC* in water balance modeling at various timescales and under different climate conditions; and (3) to identify the dominant climatic controlling factors on the modeling errors of the Budyko framework. It is anticipated that the knowledge obtained from this study would enhance understanding of the controls of climatic and catchment characteristics on the water balances from arid to humid climates and across a variety of timescales.

2 Methodology

2.1 Data sources

A long-term (1960–2008) meteorological and hydrologic gridded dataset, covering the entire China with a 0.25 ° spatial resolution, is provided by Zhang et al. (2014). The observed meteorological data, including *P*, maximum temperature T_{max}, minimum temperature T_{min} and wind speed *WS*, are derived from the total 756 monitoring stations maintained by the Chinese Meteorological Administration (CMA). The hydrologic flux data including *E*, surface runoff (R_s) and baseflow (B_s), are obtained from the Variable Infiltration Capacity (VIC) model simulation forced by daily observed climate forcing data of *P*, T_{max}, T_{min}, and *WS*. The dataset used here provides a more reliable estimate of *R*, *E* and other hydrologic variables over China compared with the global products of a similar nature (e.g., Nijssen et al., 2001; Adam et al., 2006; Rodell et al., 2004; Sheffield et al., 2006; Sheffield and Wood, 2007; Pan et al., 2012), and hence it will be treated and termed as the "observed data" in this paper, particularly in contrast to the "predicted data" from the Budyko models. This dataset has been successfully used for the quantitative assessment of effects of climate and *WSC* on the temporal variability of actual evapotranspiration in China (Wu et al., 2017). The *PET* data spanning the period 1960–2008 with a 1 °resolution is provided by the Hydroclimatology Group of Princeton University (Sheffield et al., 2006, 2012). The *PET* is estimated based on the Penman equation (Penman, 1948; Shuttleworth, 1993) using the updated meteorological dataset obtained from Sheffield et al. (2006, 2012).

All the data used are disaggregated into 0.5° × 0.5° grids over China (for a total of 3814 grids) using the linear interpolation. Gridded *WSC* at the time interval dt_i is computed using the water balance equation:

$$dS_i / dt_i = P_i - E_i - R_{si} - B_{si} \quad (1)$$

Hydrol. Earth Syst. Sci. Discuss., https://doi.org/10.5194/hess-2017-441
Manuscript under review for journal Hydrol. Earth Syst. Sci.
Discussion started: 25 August 2017

A total of 14 large river basins in China under a large diversity of climates, are chosen for analysis (Figure 1(a)). The monthly and annual P, E, R_s, B_s and PET for each of the 14 basins are estimated from the grid data within the basin boundary. The basic and detailed information of the 14 basins and their long-term (1960–2008) mean water balances are given in Table 1. As seen, the mean annual aridity index (PET/P) is less than 1.0 in the Southeast Drainage, Pearl and Yangtze River basins belonging to humid climates, and in the range of 1.19–8.63 for the other eleven basins belonging to arid climates.

The net primary productivity (NPP) is an important component of the global carbon budget directly reflecting the production capacity of vegetation, and it is the basis of organic material and energy cycles in the global ecosystem (Field et al. 1998; Houghton et al. 1999; Field, 2001). The formation of NPP can effectively indicate the ecological response of catchment characteristics. In this study, the 1-km NPP data set in 2010 covering the entire China as obtained from the Research Center for Natural resources and Environment Science Data of the Chinese Academy of Science, is used to represent the vegetation characteristics of catchments over China. Figure 1(b) show the spatial distribution of NPP over China. The value of NPP generally decreases from southern to northwest China, which is generally opposite to the pattern of mean annual aridity index. Scatterplot of NPP versus the mean annual aridity index for the 3814 grids of China is shown in Figure 1(c). As seen, the NPP decreases rapidly with the increasing aridity index for all regions with the aridity index smaller than 3. However, under the extremely dry conditions (the aridity index > 3) the NPP falls within a narrow range fluctuating around zero. NPP is negligible in the extremely dry regions such as some regions of Xinjiang.

2.2 Dry and wet seasons

For a given catchment, the dry and wet months among the twelve months of a year are identified based on the mean monthly aridity index expressed as (Chen et al., 2013)

$$A_m = \frac{\overline{PET_m}}{\overline{P_m} - \overline{\frac{dS_m}{dt_m}}} \tag{2}$$

where $\overline{PET_m}$, $\overline{P_m}$ and $\overline{\frac{dS_m}{dt_m}}$ are the 1960–2008 monthly climatology of potential evaporation, precipitation and storage

Hydrol. Earth Syst. Sci. Discuss., https://doi.org/10.5194/hess-2017-441
Manuscript under review for journal Hydrol. Earth Syst. Sci.
Discussion started: 25 August 2017

change, respectively. The classification between dry and wet months are based upon the criterion of $A_m \geq 1$ (dry) or $A_m < 1$ (wet) for each month from January through December, and this classification remains the same for all years. Based on the identified dry and wet months, the dry and wet seasonal precipitation, potential evaporation, and storage changes are calculated by summing up the dry- and wet-months values for each year during 1960–2008. For example, the dry seasonal *PET* (PET_d) and the wet seasonal *PET* (PET_w) are computed as

$$PET_d = \sum_{i=1}^{N_d} PET_{d,i}$$
$$PET_w = \sum_{i=1}^{N_w} PET_{w,i} \quad (3)$$

where N_d and N_w represent the numbers of dry and wet months within a year (i.e. $N_d + N_w = 12$).

2.3 The Budyko model (BM)

The Budyko curves are the equations coupling the concepts of water and energy balances which usually contain one or more parameters to be estimated (Turc, 1954; Pike, 1964; Fu, 1981; Choudhury, 1999, Zhang et al., 2001, 2004; Porporato et al., 2004; Yang et al., 2008; Gerrits et al., 2009). One of the commonly used functional forms is the Fu's equation (Fu, 1981; Zhang et al., 2004) expressed as follows:

$$\frac{E}{P} = 1 + \frac{PET}{P} - [1 + (\frac{PET}{P})^{\omega}]^{1/\omega} \quad (4)$$

where the parameter ω represents the effects of land surface characteristics and climate seasonality on the water-energy balance (Li et al., 2013). The Fu's equation with a clear physical basis is considered to be more applicable for estimating mean annual evapotranspiration than other empirical formulas (Zhang et al., 2004).

As the timescale becomes finer, *WSC* becomes more significant in closing water budget since it controls the supply and demand of water fluxes with a delayed effect (Chen et al. 2013). Therefore, the effect of *WSC* has to be incorporated into BM particularly when applied to smaller timescales. Following Wang (2012), the water availability is defined as the effective

precipitation P_e, (i.e., $P_e = P - dS/dt$), thus Equation (4) becomes (Zeng and Cai, 2015)

$$\frac{E}{P_e} = 1 + \frac{PET}{P_e} - [1 + (\frac{PET}{P_e})^{\omega}]^{1/\omega} \quad (5)$$

In this study, both equations (4) and (5) will be applied to the smaller timescales (i.e. annual, seasonal and monthly). The parameters ω is estimated by using the least-square method.

2.4 Model performance evaluation

The model performance is evaluated by using the Nash-Sutcliffe Coefficient of Efficiency (*CE*) and the Relative Error (*RE*). The *CE* is calculated as

$$CE = 1 - \frac{\sum_{i=1}^{N}(E_{o,i} - E_{s,i})^2}{\sum_{i=1}^{N}(E_{o,i} - \overline{E}_{o,i})^2} \quad (6)$$

where $E_{o,i}$ and $E_{s,i}$ are the observed and simulated *E* at the *i*th time step, respectively. *N* is the number of the time steps. *CE* ranges from $-\infty$ to 1. A positive *CE* value indicates acceptable model performance, and a *CE* closer to 1 indicates more efficient model performance (Moriasi et al., 2007).

The *RE* is a percentage measurement of mean bias of model simulations relative to observations, defined as

$$RE = \frac{\overline{E}_{s,i} - \overline{E}_{o,i}}{\overline{E}_{o,i}} \times 100\% \quad (7)$$

where $\overline{E}_{o,i}$ and $\overline{E}_{s,i}$ represent the mean observed and simulated *E* over the *N* time steps.

3 Results

3.1 Mean annual water balance

3.1.1 Basin scale

Figure 2 (a) shows the mean annual *E/P* versus *PET/P* over the 14 river basins in China. As seen, the BM (equation (4)) with

a fitted parameter ω of 1.92 adequately captures the variations in long-term water and energy balances of these basins (Figure 2a). Figure 2(c) shows the comparison between the "observed" and the BM-predicted mean annual *E* in the 14 river basins. Results indicate that the estimated *E* using the Fu's equation agrees well with observations at the long-term mean annual timescale with the correlation coefficient (*r*) of 0.97 and the *RE* of -2.9%. In addition, the estimated mean annual *E* under dry climates is more accurate than that under humid climates.

3.1.2 Grid scale

Figure 2(b) plots the mean annual *E/P* versus *PET/P* along with the distribution of NPP, while Figure 2(d) shows the comparison between observed and BM-simulated mean annual *E*. Both subplots include all the total 3814 grids in China. It is clear that most of grids follow the Budyko curve reasonably well with a fitted ω of 1.97, and the aridity index increases with the decreasing NPP. The high *r* (~0.94, Figure 2(d)) indicates that the BM can be calibrated and simulates mean annual water balance well for most grids. Consistent with the above, it is found that the model performs more accurately in the grids with a larger aridity index (i.e. smaller NPP) than more humid grids.

3.2 Annual water balance

3.2.1 Basin scale

The BM is also applied to annual water balance modeling at the basin scale. The comparison of observed and BM-simulated annual *E* in the 14 river basins is shown in Figure 3. It demonstrates that the dynamic BM model generally produces a reasonably good fit to annual *E* for most of basins. The majority of arid basins with the aridity index > 1.0 (e.g. Inner Mongolia, Qiangtang, Qinghai, Xinjiang, Hexi) have a high *CE* ranging between 0.70 and 0.97, and a small *RE* ranging between -0.11% and 0.58%, indicating the performance of BM is rather reliable in arid basins at the annual scale. In contrast, for humid basins with the aridity index < 1.0 (e.g. Southeast Drainage and Pearl, and Yangtze), although *RE* is generally small, the model fails to capture the significant interannual variability of *E* and results in a negative *CE* in Southeast Drainage and Pearl River basin.

As *WSC* can play a significant role in affecting annual *E*, the extended BM (equation (5)), which incorporates the effect of

186 *WSC* is also used to model annual water balance. The improvement relative to the original BM in the simulated annual *E* can
187 be observed from Figure 3 for the arid basins (with the aridity index > 1.0): the *CE* (*RE*) in these arid basins is ranging from
188 0.4–0.98 (-0.17% – 0.06%). However, virtually no improvement can be seen for the humid basins (Southeast Drainage, Pearl,
189 and Yangtze basins) in which the performance (*CE*) becomes worse than the BM. Therefore, the extended BM may not
190 provide significant improvement over the BM when applied to humid basins at the annual scale.

191 **3.2.2 Grid scale**

192 Similar to the basin scale, the BM for annual water balance modeling is applied to the 3814 grids over the entire China
193 (Figure 4). As seen from Figure 4a, there are 81%, 63.7% and 37.3% of grids with *CE* greater than 0, 0.5, and 0.8,
194 respectively. The *RE* for all grids ranges between -16.1% and 8.2% (Figure 4b). For the grids with the aridity index ≤ 3, *CE*
195 is considerably small under humid conditions and increases rapidly toward nearly 1.0 with the increasing aridity index
196 (Figure 4c). Similarly, *RE* is relatively large (small) under the humid (extremely dry) conditions (Figure 4e). Figure 4g
197 compares the observed and simulated interannual variability of *E* (as quantified by the standard deviation of annual *E*) for
198 the 3814 grids with the mean annual aridity index also given in the color bar. All the grids have the interannual variability of
199 *E* less than 120 mm. The correlation coefficient between observed and simulated interannual variability of *E* for all grids is
200 0.819, but the simulated *E* interannual variability is generally higher than observations (Figure 4g). Although performing
201 well for most grids in dry regions, the BM performs rather poorly for a large portion of grids in humid regions mainly due to
202 the impacts of interannual variability of *WSC* which have not been included in the BM.
203
204 The validation of the extended BM against the observed *E* (red line in Figure 4a) indicates that 83.5%, 70.1% and 48.1% of
205 grids with the *CE* > 0, 0.5 and 0.8, respectively. The *RE* ranges between -16.1% to 6.9% (Figure 4b) rather close to the
206 performance of BM. The correlation coefficient between observed and simulated interannual variability of *E* is 0.835,
207 slightly larger than 0.819 of the BM. However, the overestimated interannual variability of *E* in BM in humid grids is
208 significantly improved by the extended BM (Figure 4h). Overall the extended BM provides potential improvements of
209 annual water balance at the grid scale mainly in correcting the overestimated interannual variability of *E*, but the
210 improvement is limited for the grids with the underestimated interannual variability (Figures 4g and 4h).

Hydrol. Earth Syst. Sci. Discuss., https://doi.org/10.5194/hess-2017-441
Manuscript under review for journal Hydrol. Earth Syst. Sci.
Discussion started: 25 August 2017

3.3 Seasonal water balance

3.3.1 Basin scale

Following the definition of the wet- and dry-season (equations (2) and (3)), the wet and dry seasonal PET/P, PET/P_e, E/P, and E/P_e are calculated respectively in each basin. For some extremely humid (arid) basins, the mean monthly aridity indices can be all smaller (larger) than 1.0 for all twelve months so that there is only wet (dry) season without any dry (wet) season. Figure 5 shows the validation of the BM and extended BM against observed E at the dry seasonal scale for all 13 basins except the Southeast Drainage basin which does not have any dry season. As seen, the BM performs poorly in capturing the peaks and troughs of E in the Pearl, Yangtze, Southwest Drainage and Huaihe basins, with the CE all below 0.4. For the other 9 less humid basins in Figure 5, the simulated E by the BM agrees well with observed E with the CE (RE) ranging from 0.52 to 0.97 (0.02% and 0.24%). Significant improvements in the extended BM simulations are found for all basins, particularly notable in the Pearl, Southwest Drainage, Huaihe and Liaohe basins. The CE of the extended BM ranges between 0.44–0.98, and there are seven out of 13 basins with $CE > 0.9$, indicating that the extended BM simulation is generally accurate in the dry seasonal scale.

The validations of the BM and extended BM against observed E in the wet seasonal scale are shown in Figure 6 for the only 8 out of the 14 basins with the wet season. As seen, the BM is unable to simulate E accurately with all CE less than 0.5. Similar to that found in the BM simulation, the extended BM simulations still show large discrepancy in reproducing the observed interannual variability of E at the wet seasonal scale. Particularly for the Huaihe basin, both the BM and the extended BM significantly underestimate the long-term mean E, with the RE –10.93% and –10.33% respectively. The simulated E cannot well capture the sharp rises and falls of interannual variability of E, likely due to the strong variability of water balance at the wet seasonal scale.

3.3.2 Grid scale

Similar to the basin scale, the PET/P, PET/P_e, E/P and E/P_e are calculated separately for wet- and dry-season at the grid scale. The validation of the BM and extended BM against observed E in dry season for the selected grids is shown in Figure 7. There are 3538 out of the total 3814 grids (92.8%) with dry season identified within twelve months. For the performance

of BM, the *CE* is larger than 0, 0.5 and 0.8 for 83.1%, 64.5% and 39.9% of grids, respectively. The *CE* is small in humid grids and increases as the aridity index increases. When moving toward increasingly drier climates, the *CE* gradually becomes insensitive to the aridity index (> 20) and approaches to the upper limit of 1.0. Strong correlation (~0.94) is found between the observed and simulated interannual variability of *E* in dry season (Figure 7g). However, the BM tends to overestimate the interannual variability of *E* particularly for the humid basins with the *RE* as large as 124.3% (Figure 7e). The results suggest that the BM is more applicable to arid than humid climates, similar to that found in analyzing annual water balance. The validation of the extended BM performance against observed *E* indicates a significant improvement over the BM. There are more than 96.3%, 85.4%, and 60% of grids with *CE* > 0, 0.5 and 0.8, respectively. The *RE* in humid climates is reduced from >100% in BM to only about 10–20% in the extended BM (Figure 7f), also the overestimated variability of simulated *E* in humid climates is largely corrected by the extended BM (Figure 7h) to achieve excellent performance in water balance modeling in dry season.

The validation of the BM and extended BM against observed *E* in the wet season at the grid scale is shown in Figure 8. There are in total 1982 out of 3814 grids (52%) with the wet season identified within twelve months. For these 1982 grids, the *CE* of the BM simulation are all < 0.73, and only 41.3% of grids with *CE* > 0. The *RE* of the BM simulation is negative for 83.4% of grids, and it tends to perform even worse in more arid climates (Figure 8e). Based on these results, it can be concluded that the BM performance is not satisfactory in the wet season at the grid scale, similar to that found at the basin scale. The performance of the extended BM in the wet season is similarly poor as the BM for most grids. Therefore, more sophisticated water balance models with the capability of simulating important mechanisms in wet season are required to model the interannual variability of water balance more accurately for all basins and grids under diverse climates.

3.4 Monthly water balance

3.4.1 Basin scale

The BM and the extended BM are applied to model monthly water balance for the 14 river basins. The comparisons between the observed and simulated monthly *E* from both models are presented in Figure 9. Overall, the BM performs well in all basins with the *RE* (*CE*) between –16.6% and 9.5% (0.69 and 0.98). However, the BM tends to underestimate the peaks of *E*

261 in some basins (Southeast Drainage, Pearl, Yangtze, Southwest Drainage and Huaihe). In contrast, the extended BM
262 performs poorly for most basins (particularly in humid basins), with 8 out of 14 basins having *CE* lower than the BM and 11
263 out of 14 basins having the absolute value of *RE* larger than the BM. Improvements caused by using the extended BM can
264 only be found in several dry basins (e.g., Qinghai, Xinjiang, and Hexi).

265 **3.4.2 Grid scale**

266 The validation of the BM and the extended BM against observed *E* at the monthly scale is presented in Figure 10. For the
267 BM, there are 97.1% and 57.2% of the 3814 grids with the $CE > 0$ and 0.8, respectively. For the extended BM, almost all the
268 grids have $CE > 0$ and 68.1 % of grids have $CE > 0.8$. The *RE* in the BM (the extended BM) ranges between –40.8% and
269 449.5% (–49.6% and 72.2%). The BM tends to be more accurate in arid climates, consistent with the findings at the annual
270 and seasonal timescales. However, the extended BM performs poorly in arid climates, significantly underestimating the
271 intra-annual variability of *E* in humid climates (Figure 10h). Comparisons between Figure 10c and 10d reveal that the BM
272 performs better performance (with larger *CE*) than the extended BM mainly in the grids with the aridity index > 20, while
273 the extended BM performs better than BM mainly in the grids with a smaller aridity index (< 10).

274 **4. Discussion**

275 **4.1 The role of water storage change (*WSC*) in water balance modeling**

276 In general, the influence of *WSC* is more significant in the annual and smaller timescales (Wu et al., 2017), and this has been
277 recognized to have an impact on the water balance modeling of BM (Zhang et al., 2008; Donohue et al., 2010; Chen et al.,
278 2013). Figure 11 plots the mean variability (i.e. standard deviation) of the modeling errors of BM (the simulated minus the
279 observed *E*) versus the mean variability (i.e. standard deviation) of *WSC* from the annual, dry season, wet season and
280 monthly timescales. As seen, both the variability of the modeling errors in *E* and the variability of *WSC* are larger under
281 more humid climates. The variability of modeling errors in *E* shows a strong positive correlation (ranging from 0.6 to 0.8)
282 with that of *WSC* for all the four timescales examined. In addition, the correlation tends to be stronger in dry season (Figure
283 11b) than in wet season (Figure 11c).
284

Hydrol. Earth Syst. Sci. Discuss., https://doi.org/10.5194/hess-2017-441
Manuscript under review for journal Hydrol. Earth Syst. Sci.
Discussion started: 25 August 2017

Hydrology and Earth System Sciences
Discussions

Figure 12 shows the relations between *CE* and σ_{WSC}/σ_E (the ratio between the standard deviations of observed *WSC* and *E*) at four different timescales. As shown, *WSC* is significant on the variability of water balance at annual and smaller timescales (particularly at the seasonal timescale) and the variability of *WSC* tends to be more significant than that of *E* in humid climates. The correlation coefficients of *CE* and σ_{WSC}/σ_E range between –0.67 and –0.44 at four timescales, indicating that a larger σ_{WSC}/σ_E would lead to low accuracy in the BM simulations particularly in humid climates. These results suggest that the BM is not suitable for water balance modeling in humid climates at the smaller timescales when the temporal variability of *WSC* is significant.

4.2 Primary controlling factors in the modeling errors of BM in humid climates

As mentioned before, the BM performs poorly in humid climates with large modeling errors over the long-term mean annual, annual, seasonal, and monthly timescales. In humid climates, the partitioning of *P* into *E* and runoff is mainly controlled by *PET*, which is commonly termed as the energy-limited condition (Zhang et al., 2004, 2008; Yang et al., 2009, Zeng and Cai, 2015). Therefore, the performance of the BM in modeling *E* should be dependent on both *PET* and *E* under the energy-limited condition.

According to McVicar et al. (2012), the climate conditions can be classified into three cases: the energy-limited areas (mean annual aridity index < 0.76), the 'equitant' areas (0.76 < mean annual aridity index < 1.35), and the water-limited areas (mean annual aridity index > 1.35). In this study, a total of 622 grids categorized as the energy-limited condition with mean annual aridity index < 0.76 are identified from the total 3814 grids in China. The *RE* of the BM simulations for each of the 622 grids at mean annual, annual, seasonal, and monthly timescales are compared with the mean ratio of *PET*/*E* in Figure 13. As seen, the mean *RE* is generally smaller than zero at all mean annual, annual, seasonal, and monthly timescales when the mean *PET*/*E* < 1.5. It is clear that the mean *RE* is positively correlated with the mean *PET*/*E*, particularly at the mean annual scale with a large correlation coefficient of 0.976. The pattern of the scatterplot at the annual scale is similar to that at the wet seasonal scale. When the mean *PET*/*E* < 1.5, the mean *RE* is sensitive to the mean *PET*/*E*. However, when the mean *PET*/*E* > 1.5, the mean *RE* becomes insensitive to the mean *PET*/*E* and falls within a narrow range fluctuating around zero. As the timescale decreases to the month scale, the mean *RE* tends to become large with the increasing mean *PET*/*E* when the mean

310 *PET*/*E* > 1.5. Overall the mean *RE* is strongly correlated with the mean *PET*/*E* at the monthly timescale, and this is likely
311 due to the in-phase seasonality between *PET* and *E* under the energy-limited condition. The results suggest that the *PET*/*E*
312 (especially for the condition *PET*/*E* < 1.5) can be one of the main factors controlling the errors of the BM simulation under
313 the energy-limited condition.

314 **5 Summary and future work**

315 On the basis of a long-term (1960–2008) land surface hydrologic data, this paper presents a systematic examination of the
316 applicability of the Budyko framework at four temporal scales (long-term mean annual, annual, seasonal, and monthly)
317 under a wide variety of climatic conditions in China. The original Budyko model and the extended Budyko model (which
318 incorporates the effect of *WSC* by using the effective precipitation *P*-*WSC* to replace *P*) are validated at both the 14 river
319 basins and the total 3814 0.5° × 0.5° grid scales for the entire China. The role of *WSC* in modeling water balance and the
320 dominant climate factors controlling the modeling errors of *E* by the original Budyko model are emphasized.
321
322 At the long-term mean annual scale which the effect of *WSC* is negligible, the Budyko model generally performs well in
323 terms of simulated *E*, and the performance in arid climates is better than that in humid climates. The effect of *WSC* becomes
324 significant in modeling *E* at the smaller temporal scales particularly in humid climates. Under such circumstances, the
325 original BM is generally accurate for modeling water balance under arid climates, but it fails to capture the dominant
326 controls of *WSC* on water balance partitioning under humid climates. Overall the accuracy of the original Budyko model can
327 be ranked from high to low as follows: dry seasonal, annual, monthly, and wet seasonal scales. As the effective precipitation
328 is used as a substitute for precipitation in the extended Budyko model, an improvement of water balance modeling can be
329 found in arid climates, but to a much lesser extent in humid climates. The performance of the extended Budyko model is
330 generally better than the original Budyko model at the dry seasonal timescale, but tends to be worse at both the wet seasonal
331 and monthly timescales. More sophisticated models explicitly accounting for the effect of *WSC* are required to improve
332 water balance modeling particularly in humid climates and at smaller timescales.
333
334 The *WSC* and the modeling errors in *E* both show larger temporal variability in humid climates. The temporal variability of

335 modeling errors in *E* shows a strong positive correlation with that of *WSC* at all annual, seasonal and monthly timescales (the
336 correlation coefficient between 0.6–0.8, Figure 11). The accuracy of the Budyko model simulations decrease with the
337 increased ratio between the standard deviations of *WSC* and *E* particularly in humid climates. In addition, under the
338 energy-limited condition (mainly in humid climates), the mean relative errors of the Budyko model show a strong positive
339 correlation with the mean ratio of *PET*/*E* at the long-term mean annual timescale. However, at the annual and seasonal
340 timescales, the mean relative errors are sensitive to the mean ratio of *PET*/*E* only under the condition *PET*/*E* < 1.5. Future
341 research will be focused on the identification and quantifications of controlling factors in the modeling errors of the Budyko
342 model from the arid to humid climates over variable timescales, particularly when *PET*/*E* is greater than 1.5.

343 **Acknowledgements**

344 This work was supported by the Fundamental Research Funds for the Central Universities (Grant No. 21617301) and the
345 Open Project Program of Chongqing Key Laboratory of Karst Environment (Grant No. Cqk 201702), and partly supported
346 by the National Natural Science Foundation of China (Grant No. 41530316) and the National Key Research and
347 Development Program of China (Grant No. 2016YFC0402805).

348 **References**

349 Adam, J. C., Clark, E. A., Lettenmaier, D. P., and Wood, E. F.: Correction of global precipitation products for orographic
350 effects, J. Climate., 19, 15–38, 2006.
351 Budyko, M. I.: The Heat Balance of the Earth's Surface, 259 pp., U.S. Dep. of Commer., Washington, D. C, 1958.
352 Budyko, M. I.: Climate and Life. Elsevier, New York, 1974.
353 Carmona, A. M., Sivapalan, M., Yaeger, M. A., and Poveda, G.: Regional patterns of interannual variability of catchment
354 water balances across the continental U.S.: A Budyko framework, Water Resour. Res., 50, 9177–9193, 2014.
355 Chen, X., Alimohammadi, N., and Wang, D.: Modeling interannual variability of seasonal evaporation and storage change
356 based on the extended Budyko framework, Water Resour. Res., 49, doi :10.1002/wrcr.20493, 2013.
357 Cheng, L., Xu, Z., Wang, D., and Cai, X.: Assessing interannual variability of evapotranspiration at the catchment scale

using satellite-based evapotranspiration data sets, Water Resour. Res., 47, W09509, doi:10.1029/2011WR010636, 2011.

Choudhury, B. J.: Evaluation of an empirical equation for annual evaporation using field observations and results from a biophysical model, J. Hydrol. 216, 99–110, 1999.

Du, C., Sun, F., Yu, J., Liu, X., and Chen, Y.: New interpretation of the role of water balance in an extended Budyko hypothesis in arid regions, Hydrol. Earth Syst. Sci., 20(1), 393–409, 2016.

Donohue, R. J., Roderick, M. L., and McVicar, T. R.: On the importance of including vegetation dynamics in Budyko's hydrological model, Hydrol. Earth Syst. Sci., 11, 983–995, doi:10.5194/hess-11-983-2007, 2007.

Donohue, R. J., Roderick, M. L., and McVicar, T. R.: Can dynamic vegetation information improve the accuracy of Budyko's hydrological model?, J. Hydrol., 390(1–2), 23–34, 2010.

Donohue, R. J., Roderick, M. L., and McVicar, T. R.: Assessing the differences in sensitivities of runoff to changes in climatic conditions across a large basin, J. Hydrol., 406, 234–244, doi:10.1016/j.jhydrol.2011.07.003, 2011.

Eltahir, E. A. B, and Yeh, P. J. -F.: On the Asymmetric Response of Aquifer Water Level to Droughts and Floods in Illinois, Water Resour. Res., 35(4), 1199–1217, 1999.

Field, C. B.: Sharing the garden, Science, 294, 2490–2491, 2001.

Field, C. B., Behrenfeld, M. J., Randerson, J. T.: Primary production of the biosphere: integrating terrestrial and oceanic components, Science, 281, 237–240, 1998.

Fu, B.: The calculation of the evaporation from land surface, Sci. Atmos. Sin., 5(1), 23–31, 1981. (in Chinese).

Gerrits, A. M. J., Savenije, H. H. G., Veling, E. J. M., and Pfister, L.: Analytical derivation of the Budyko curve based on rainfall characteristics and a simple evaporation model, Water Resour. Res., 45, W04403, doi:10.1029/2008WR007308, 2009.

Houghton, R. A., Hackler, J. L., and Lawrence, K. T.: The U.S. carbon budget contributions from land-use change, Science, 285, 574–578, 1999.

Istanbulluoglu, E., Wang, T., Wright, O. M., and Lenters, J. D.: Interpretation of hydrologic trends from a water balance perspective: The role of groundwater storage in the Budyko hypothesis, Water Resour. Res., 48, W00H16,

382 doi:10.1029/2010WR010100, 2012.

383 Koster, R. D., and Suarez, M. J.: A simple framework for examining the interannual variability of land surface moisture
384 fluxes, J. Clim., 12(7), 1911–1917, 1999.

385 Li, D., Pan, M., Cong, Z., Zhang, L., and Wood, E.: Vegetation control on water and energy balance within the Budyko
386 framework, Water Resour. Res., 49, 969–976, doi :10.1002/wrcr.20107, 2013.

387 McVicar, T. R., Roderick, M. L., Donohue, R. J., and Van Niel, T. G.: Less bluster ahead? Ecohydrological implications of
388 global trends of terrestrial near-surface wind speeds, Ecohydrol., 5, 381–388, doi: 10.1002/eco.1298, 2012.

389 Moriasi, D. N., Arnold, J. G., Van Liew, M. W., Bingner, R. L., Harmel, R. D., and Veith, T. L.: Model evaluation guidelines
390 for systematic quantification of accuracy in watershed simulations, Trans. ASABE, 50(3), 885–900, 2007.

391 Nijssen, B., Schnur, R., and Lettenmaier, D. P.: Global retrospective estimation of soil moisture using the Variable Infiltration
392 Capacity land surface model, 1980–93, J. Climate., 14, 1790–1808, 2001.

393 Oudin, L., Andr éssian, V., Lerat, J., and Michel, C.: Has land cover a significant impact on mean annual streamflow? An
394 international assessment using 1508 catchments, J. Hydrol., 357(3–4), 303–316, doi:10.1016/j.jhydrol.2008.05.021, 2008.

395 Pan, M., Sahoo, A. K., Troy, T. J., Vinukollu, R. K., Sheffield, J., and Wood, E. F.: Multisource estimation of long-term
396 terrestrial water budget for major global river basins, J. Climate., 25, 3191–3206, 2012.

397 Peel, M. C., McMahon, T. A., and Finlayson, B. L.: Vegetation impact on mean annual evapotranspiration at a global
398 catchment scale, Water Resour. Res., 46, W09508, doi:10.1029/2009WR008233, 2010.

399 Penman, H. L.: Natural evaporation from open water, bare soil and grass, Proc. Roy. Soc. Lond., 193, 120–145, 1948.

400 Pike, J. G.: The estimation of annual runoff from meteorological data in a tropical climate, J. Hydrol., 2, 116–123, 1964.

401 Porporato, A., Daly, E., and Rodriguez-Iturbe, I.: Soil water balance and ecosystem response to climate change, Am. Nat.,
402 164(5), 625–632, 2004.

403 Potter, N. J., and Zhang, L.: Interannual variability of catchment water balance in Australia, J. Hydrol. 369, 120–129, 2009.

404 Rodell, M., and Coauthors: The Global Land Data Assimilation System, Bull. Amer. Meteor. Soc., 85, 381–394, 2004.

405 Roderick, M. L., and Farquhar, G. D.: A simple framework for relating variations in runoff to variations in climatic
406 conditions and catchment properties, Water Resour. Res., 47, doi:10.1029/2010WR009826, 2011.

407 Sankarasubramanian, A., and Vogel, R. M.: Annual hydroclimatology of the United States, Water Resour. Res., 38(6), 1083,
408 doi:10.1029/2001WR000619, 2002.
409 Sheffield, J., Goteti, G., and Wood, E. F.: Development of a 50-year high-resolution global dataset of meteorological forcings
410 for land surface modeling, J. Climate., 19, 3088–3110, 2006.
411 Sheffield, J., and Wood, E. F.: Characteristics of global and regional drought, 1950–2000: Analysis of soil moisture data from
412 off-line simulation of the terrestrial hydrologic cycle, J. Geophys. Res., 112, D17115, doi: 10.1029/2006JD008288, 2007.
413 Sheffield, J., Wood, E. F., and Roderick, M. L.: Little change in global drought over the past 60 years, Nature, 491, 435–438.
414 doi:10.1038/nature11575, 2012.
415 Shuttleworth, W. J.: Evaporation. In: Maidment, D.R. (Ed.), Handbook of Hydrology. McGraw-Hill, Sydney, 1993.
416 Tekleab, S., Uhlenbrook, S., Mohamed, Y., Savenije, H. H. G., Temesgen, M., and Wenninger, J.: Water balance modeling of
417 Upper Blue Nile catchments using a top-down approach, Hydrol. Earth Syst. Sci., 15, 2179–2193, 2011.
418 Turc, L.: Le bilan d'eau des sols. Relations entre les precipitations, l'evaporation et l'ecoulement. Ann. Agronomy, 5, 491–
419 596, 1954.
420 Wang, D.: Evaluating interannual water storage changes at watersheds in Illinois based on long-term soil moisture and
421 groundwater level data, Water Resour. Res., 48, W03502, doi:10.1029/2011WR010759, 2012.
422 Wang, D., and Alimohammadi, N.: Responses of annual runoff, evaporation, and storage change to climate variability at the
423 watershed scale, Water Resour. Res., 48, W05546, doi:10.1029/2011WR011444, 2012.
424 Wang, D., and Hejazi, M.: Quantifying the relative contribution of the climate and direct human impacts on mean annual
425 streamflow in the contiguous United States, Water Resour. Res., 47, W00J12, doi:10.1029/2010WR010283, 2011.
426 Wang, T., Istanbulluoglu, E., Lenters, J., and Scott, D.: On the role of groundwater and soil texture in the regional water
427 balance: An investigation of the Nebraska Sand Hills, USA, Water Resour. Res., 45, W10413, doi:10.1029/2009wr007733,
428 2009.
429 Wu, C. H., Hu, B. X., Huang, G. R., and Zhang, H.: Effects of climate and terrestrial storage on temporal variability of actual
430 evapotranspiration, J. Hydrol., 594: 388–403, doi: 10.1016/j.jhydrol.2017.04.012, 2017.
431 Yang, D., Sun, F., Liu, Z., Cong, Z., Ni, G., and Lei, Z.: Analyzing spatial and temporal variability of annual water-energy

balance in nonhumid regions of China using the Budyko hypothesis, Water Resour. Res., 43, W04426, doi :10.1029/2006WR005224, 2007.

Yang, D., Shao, W., Yeh, P. J. -F., Yang, H., Kanae, S., and Oki, T.: Impact of vegetation coverage on regional water balance in the nonhumid regions of China, Water Resour. Res., 45, W00A14, doi :10.1029/2008WR006948, 2009.

Yeh, P. J. -F., and Famiglietti, J.: Regional Terrestrial Water Storage Change and Evapotranspiration from Terrestrial and Atmospheric Water Balance Computations, J. Geophys. Res., 113, doi:10.1029/2007JD009045, 2008.

Yokoo, Y., Sivapalan, M., and Oki, T.: Investigating the roles of climate seasonality and landscape characteristics on mean annual and monthly water balances, J. Hydrol., 357, 255–269, 2008.

Yu, Z., Cai, H., Yang, C., Ju, Q., Liu, D., and Sun, A.: Adaptivity of Budyko hypothesis in evaluating interannual variability of watershed water balance in Northern China, J. Hydrol. Eng., 19(4), 699–706, 2013.

Zhang, L., Dawes, W. R., and Walker, G. R.: Response of mean annual evaporation to vegetation changes at catchment scale, Water Resour. Res., 37(3), 701–708, 2001.

Zhang, L., Hickel, K., Dawes, W. R., Chiew, F. H. S., Western, A. W., and Briggs, P. R.: A rational function approach for estimating mean annual evaporation, Water Resour. Res., 40, W02502, doi:10.1029/2003WR002710, 2004.

Zhang, L., Potter, N., Hickel, K., Zhang, Y., and Shao Q.: Water balance modeling over variable time scales based on the Budyko framework—Model development and testing, J. Hydrol., 360(1–4), 117–131, 2008.

Zhang, S., Yang, H., Yang, D., and Jayawardena, A. W.: Quantifying the effect of vegetation change on the regional water balance within the Budyko framework, Geophys. Res. Lett., 43(3), 1140–1148, 2016.

Zhang, X., Tang, Q., Pan, M., and Tang, Y.: A Long-Term Land Surface Hydrologic Fluxes and States Dataset for China, J. Hydrometeor., 15, 2067–2084, doi: 10.1175/JHM-D-13-0170.1, 2014.

Zeng, R., and Cai, X.: Assessing the temporal variance of evaporation considering climate and catchment storage factors, Adv. Water Resour., 79, 51–60, 2015.

Zeng, R., and Cai, X.: Climatic and terrestrial storage control on evaporation temporal variability: Analysis of river basins around the world, Geophys. Res. Lett., 43, doi:10.1002/2015GL066470, 2016.

Hydrol. Earth Syst. Sci. Discuss., https://doi.org/10.5194/hess-2017-441
Manuscript under review for journal Hydrol. Earth Syst. Sci.
Discussion started: 25 August 2017

Hydrology and Earth System Sciences
Discussions

Table 1. Basin characteristics and long-term (1960–2008) mean water balances in the 14 river basins. *P*: precipitation, *PET*: potential evapotranspiration, *E*: evapotranspiration, *R*: streamflow, *WSC*: water storage change, *PET*/*P*: climate aridity index, *E*/*P*: evaporative efficiency

Climate type	Basin No.	Basins	*PET*/*P*	*E*/*P*	*P* (mm/year)	*PET* (mm/year)	*E* (mm/year)	*R* (mm/year)	*WSC* (mm/year)
Humid climates	1	Southeast Drainage	0.52	0.46	1790.1	936.6	817.6	973.8	-1.3
	2	Pearl	0.64	0.49	1568.1	1010.0	764.3	803.9	-0.1
	3	Yangtze	0.81	0.49	1108.3	893.1	547.0	560.9	0.4
Dry climates	4	Southwest Drainage	1.19	0.45	876.2	1040.8	398.0	471.3	6.9
	5	Huaihe	1.19	0.72	874.3	1037.7	626.2	247.5	0.6
	6	Heilongjiang	1.43	0.74	499.4	716.0	370.7	128.9	-0.2
	7	Liaohe	1.71	0.73	556.1	953.4	407.9	148.6	-0.4
	8	Haihe	2.14	0.85	535.2	1143.0	455.6	80.8	-1.2
	9	Yellow	2.38	0.74	471.0	1120.7	346.8	124.2	0.0
	10	Inner Mongolia	4.41	0.91	256.6	1132.4	233.8	22.8	0.0
	11	Qiangtang	4.70	0.82	224.9	1057.0	185.4	39.6	-0.1
	12	Qinghai	6.68	0.83	172.4	1152.2	143.5	30.7	-1.8
	13	Xinjiang	8.09	0.81	136.2	1101.7	110.4	26.9	-1.1
	14	Hexi	8.63	0.81	157.8	1362.4	128.1	31.2	-1.5

Hydrol. Earth Syst. Sci. Discuss., https://doi.org/10.5194/hess-2017-441
Manuscript under review for journal Hydrol. Earth Syst. Sci.
Discussion started: 25 August 2017

Hydrology and Earth System Sciences
Discussions
Open Access
EGU

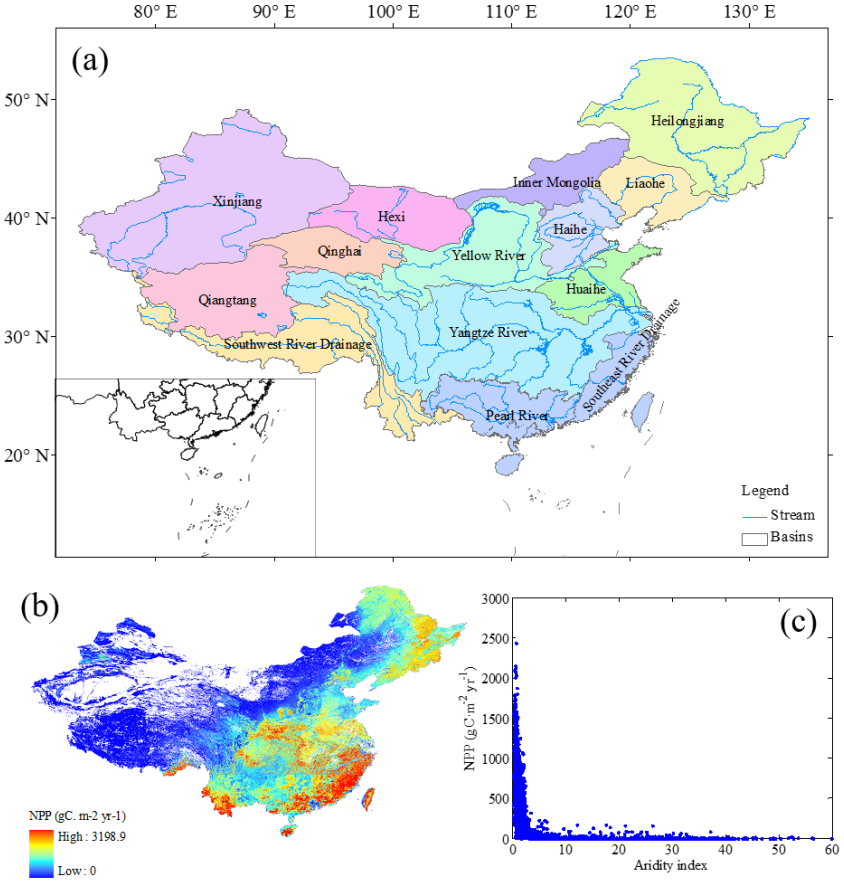

Figure 1. (a) Location of the 14 river basins in China, (b) the spatial distribution of the NPP over China, and (c) the relationship between the NPP and the aridity index for the 3814 grids over China.

Hydrol. Earth Syst. Sci. Discuss., https://doi.org/10.5194/hess-2017-441
Manuscript under review for journal Hydrol. Earth Syst. Sci.
Discussion started: 25 August 2017

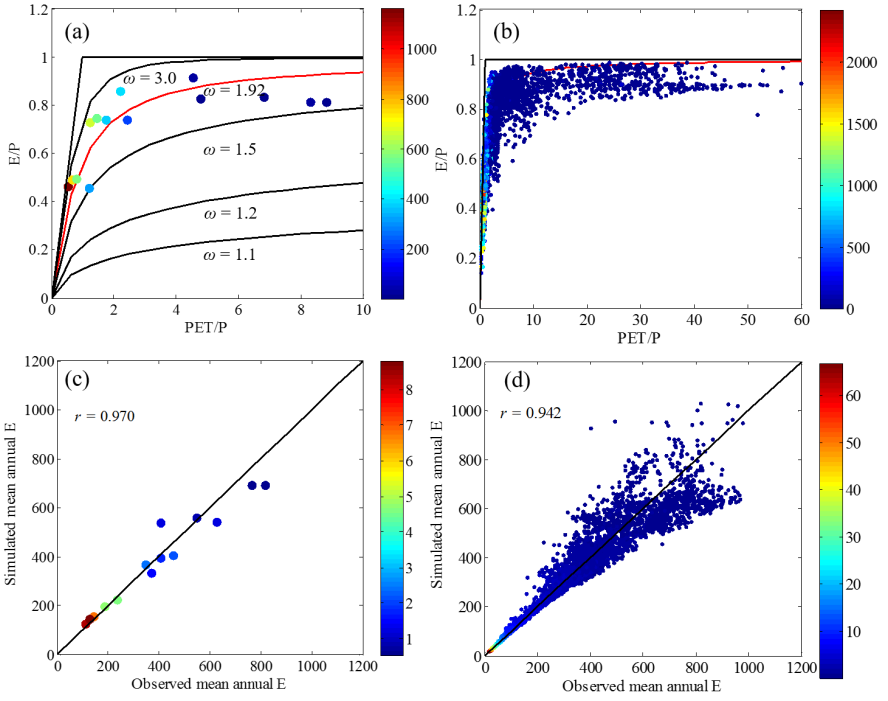

Figure 2. The mean annual evaporation ratios as a function of the mean annual aridity indices for (a) the 14 river basins and (b) the 3814 grids over China with the color bar of NPP (gC. m^{-2} yr^{-1}) for the 14 river basins and 3814 grids. The comparison of observed and simulated mean annual *E* for (c) the 14 river basins and (d) the 3814 grids over China with the color bar of the mean annual aridity index for the 14 river basins and 3814 grids. The red-lines in subplots (a) and (b) are fit by using the long-term mean data points of the 14 basins and 3814 grids, respectively.

Hydrol. Earth Syst. Sci. Discuss., https://doi.org/10.5194/hess-2017-441
Manuscript under review for journal Hydrol. Earth Syst. Sci.
Discussion started: 25 August 2017

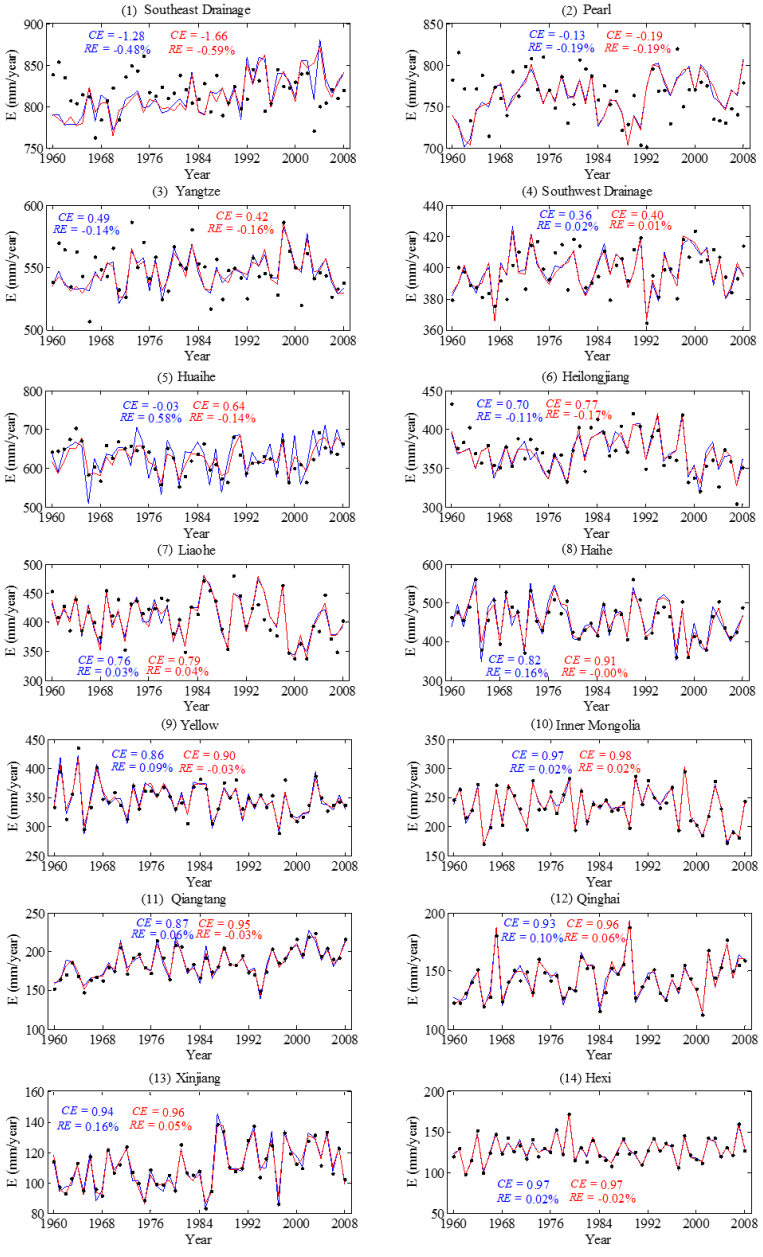

Figure 3. Comparison of annual time series of observed *E* (black dots) with that predicted by the BM (blue line) and that predicted by the extended BM (red line) for each of the 14 basins. The number in the parentheses is consistent with that given in Table 1.

Hydrol. Earth Syst. Sci. Discuss., https://doi.org/10.5194/hess-2017-441
Manuscript under review for journal Hydrol. Earth Syst. Sci.
Discussion started: 25 August 2017

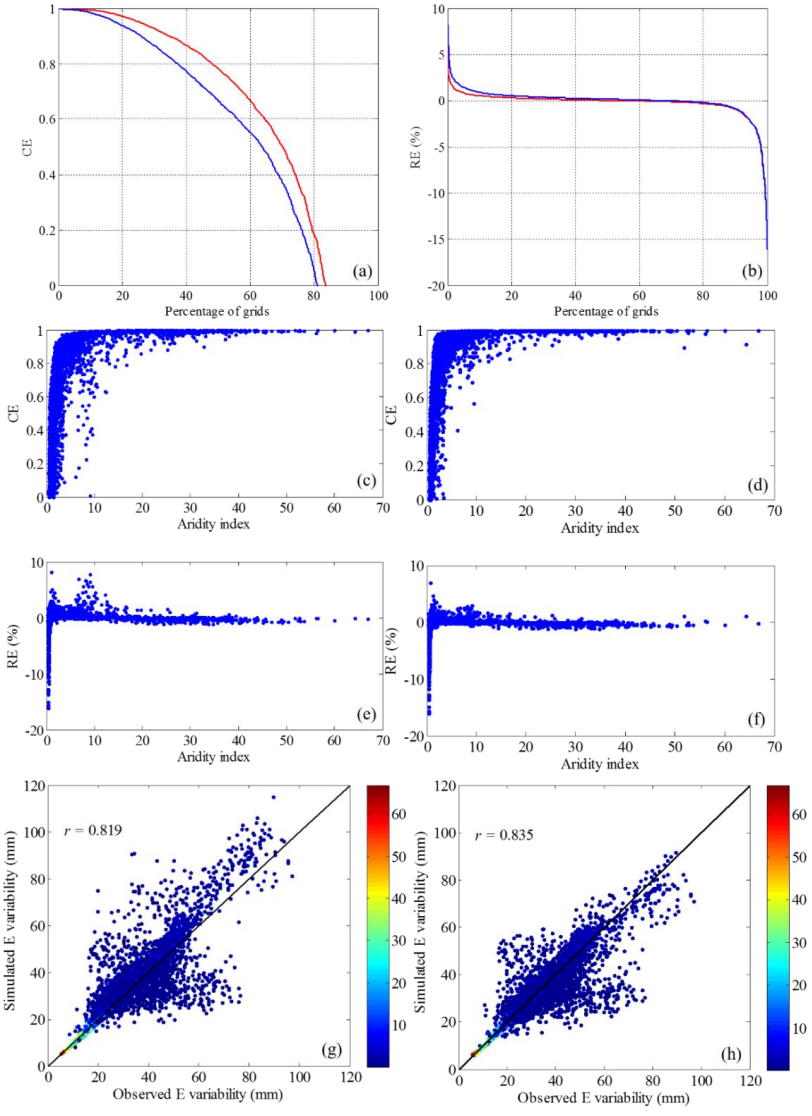

Figure 4. Model validation at the annual timescale: (a) the cumulative distribution of the percentage of grids with the *CE* larger than or equal to a specific value for the BM (blue line) and the extended BM (red line); (b) same as (a), but for *RE*. The relationship between *CE* and the aridity index for (c) the BM and (d) the extended BM for the total 3814 grids over China. The relationship between *RE* and aridity index for (e) the BM and (f) the extended BM. Comparison of observed and simulated *E* variability for (g) the BM and (h) the extended BM. The color bar indicates the mean annual aridity index for the total 3814 grids over China.

Hydrol. Earth Syst. Sci. Discuss., https://doi.org/10.5194/hess-2017-441
Manuscript under review for journal Hydrol. Earth Syst. Sci.
Discussion started: 25 August 2017

Hydrology and Earth System Sciences
Discussions

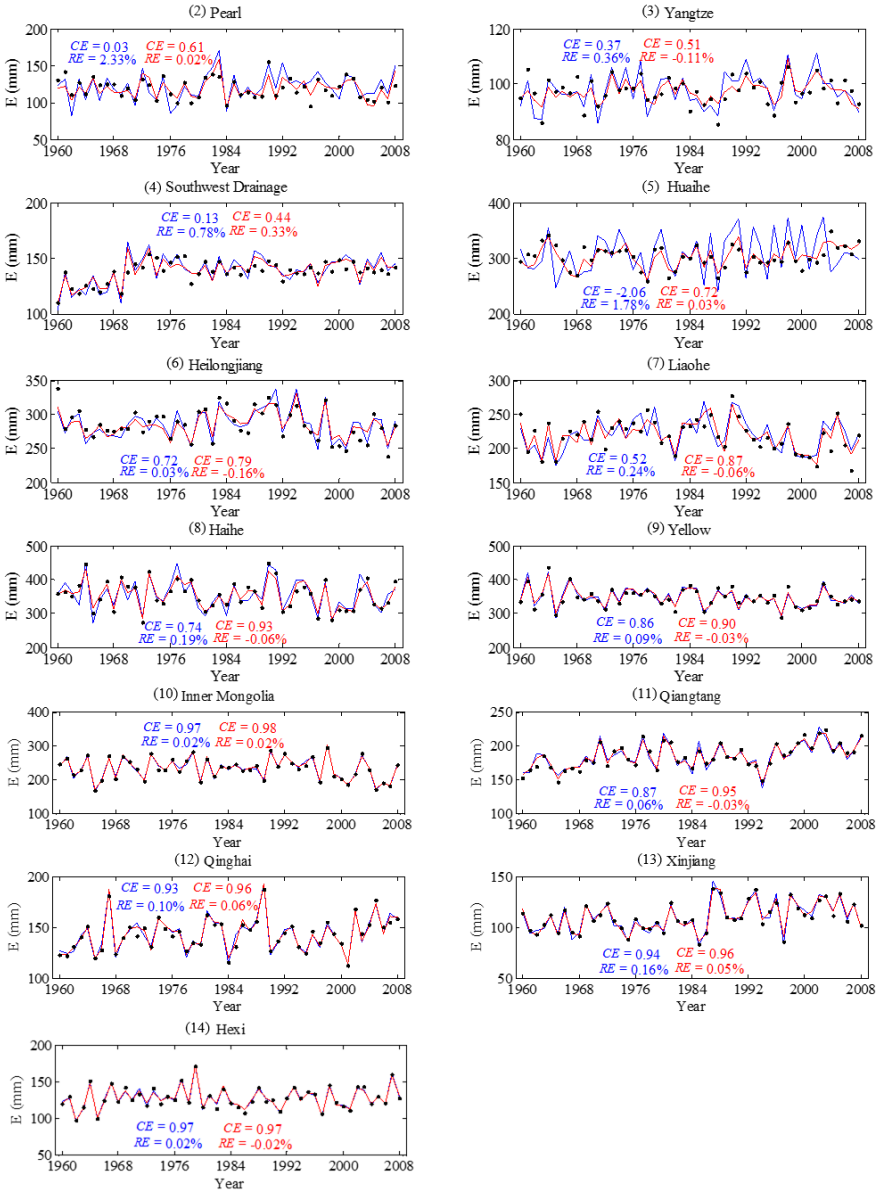

Figure 5. Comparison of dry season time series of observed *E* (black dots) with that predicted by the BM (blue line) and that predicted by the extended BM (red line) for each of the 13 basins. The number in the parentheses is consistent with that given in Table 1.

Hydrol. Earth Syst. Sci. Discuss., https://doi.org/10.5194/hess-2017-441
Manuscript under review for journal Hydrol. Earth Syst. Sci.
Discussion started: 25 August 2017

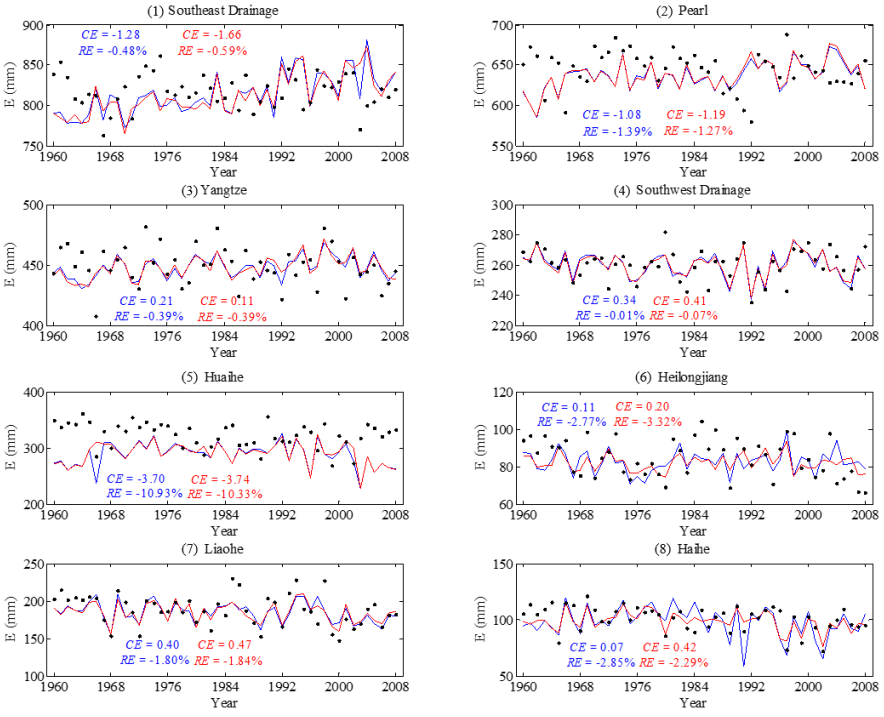

Figure 6. Comparison of wet season time series of observed *E* (black dots) with that predicted by the BM (blue line) and that predicted by the extended BM (red line) for each of the 8 basins. The number in the parentheses is consistent with that given in Table 1.

Hydrol. Earth Syst. Sci. Discuss., https://doi.org/10.5194/hess-2017-441
Manuscript under review for journal Hydrol. Earth Syst. Sci.
Discussion started: 25 August 2017

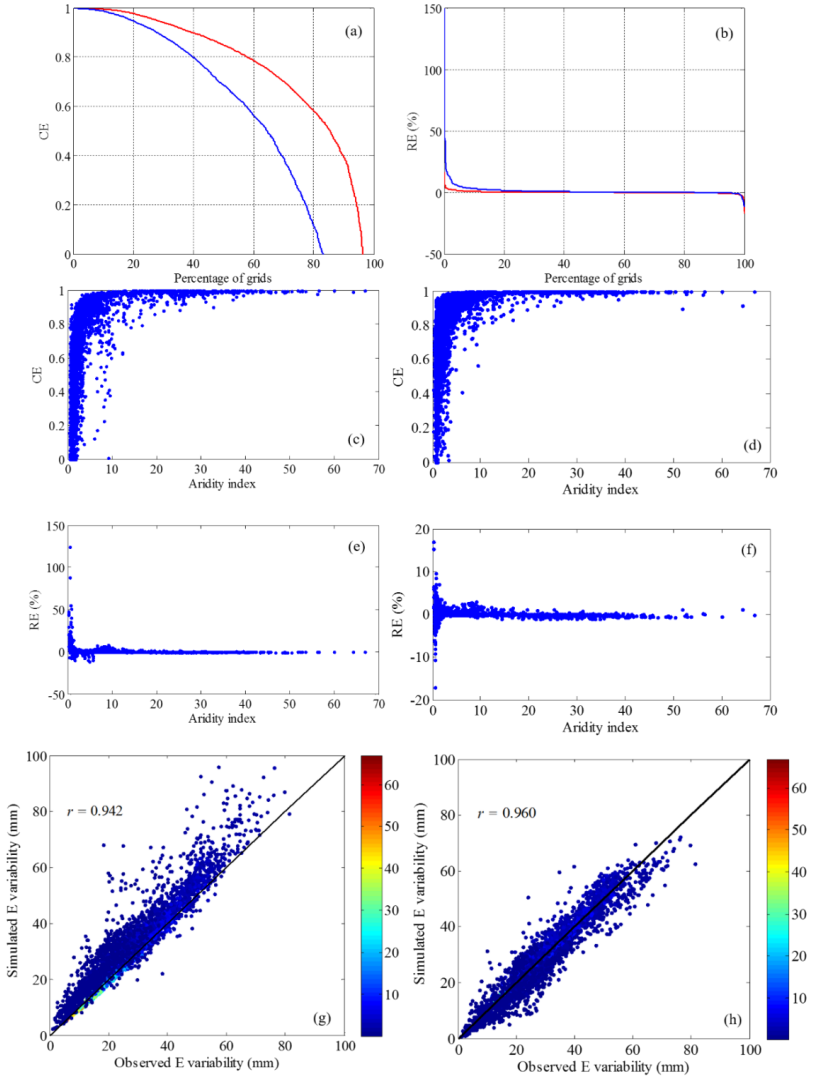

Figure 7. Model validation at the dry seasonal timescale: (a) the cumulative distribution of the percentage of grids with the *CE* larger than or equal to a specific value for the BM (blue line) and the extended BM (red line); (b) same as (a), but for *RE*. The relationship between *CE* and the aridity index for (c) the BM and (d) the extended BM for the total 3538 grids over China identified with the dry season. The relationship between *RE* and aridity index for (e) the BM and (f) the extended BM. Comparison of observed and simulated *E* variability for (g) the BM and (h) the extended BM. The color bar indicates the mean annual aridity index for the total 3538 grids over China.

Hydrol. Earth Syst. Sci. Discuss., https://doi.org/10.5194/hess-2017-441
Manuscript under review for journal Hydrol. Earth Syst. Sci.
Discussion started: 25 August 2017

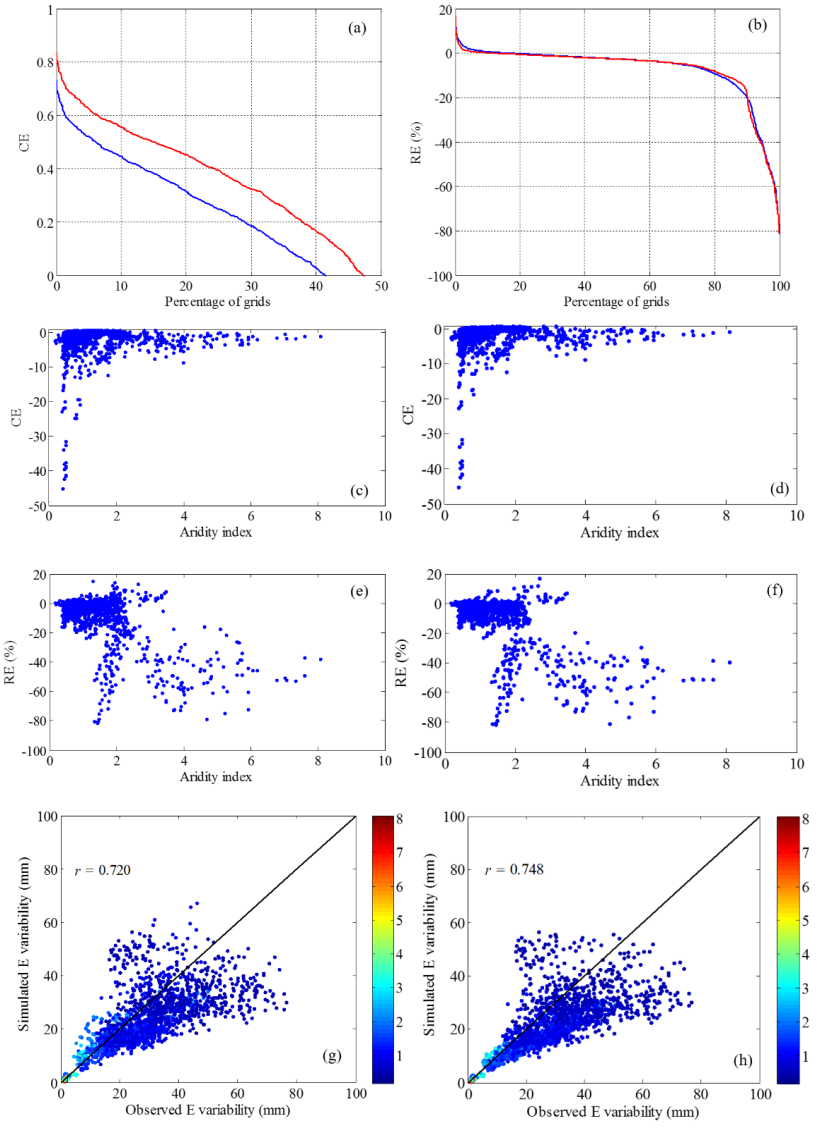

Figure 8. Model validation at the wet seasonal timescale: (a) the cumulative distribution of the percentage of grids with the *CE* larger than or equal to a specific value for the BM (blue line) and the extended BM (red line); (b) same as (a), but for *RE*. The relationship between *CE* and the aridity index for (c) the BM and (d) the extended BM for the total 1982 grids over China identified with the wet season. The relationship between *RE* and aridity index for (e) the BM and (f) the extended BM. Comparison of observed and simulated *E* variability for (g) the BM and (h) the extended BM. The color bar indicates the mean annual aridity index for the total 1982 grids over China.

Hydrol. Earth Syst. Sci. Discuss., https://doi.org/10.5194/hess-2017-441
Manuscript under review for journal Hydrol. Earth Syst. Sci.
Discussion started: 25 August 2017

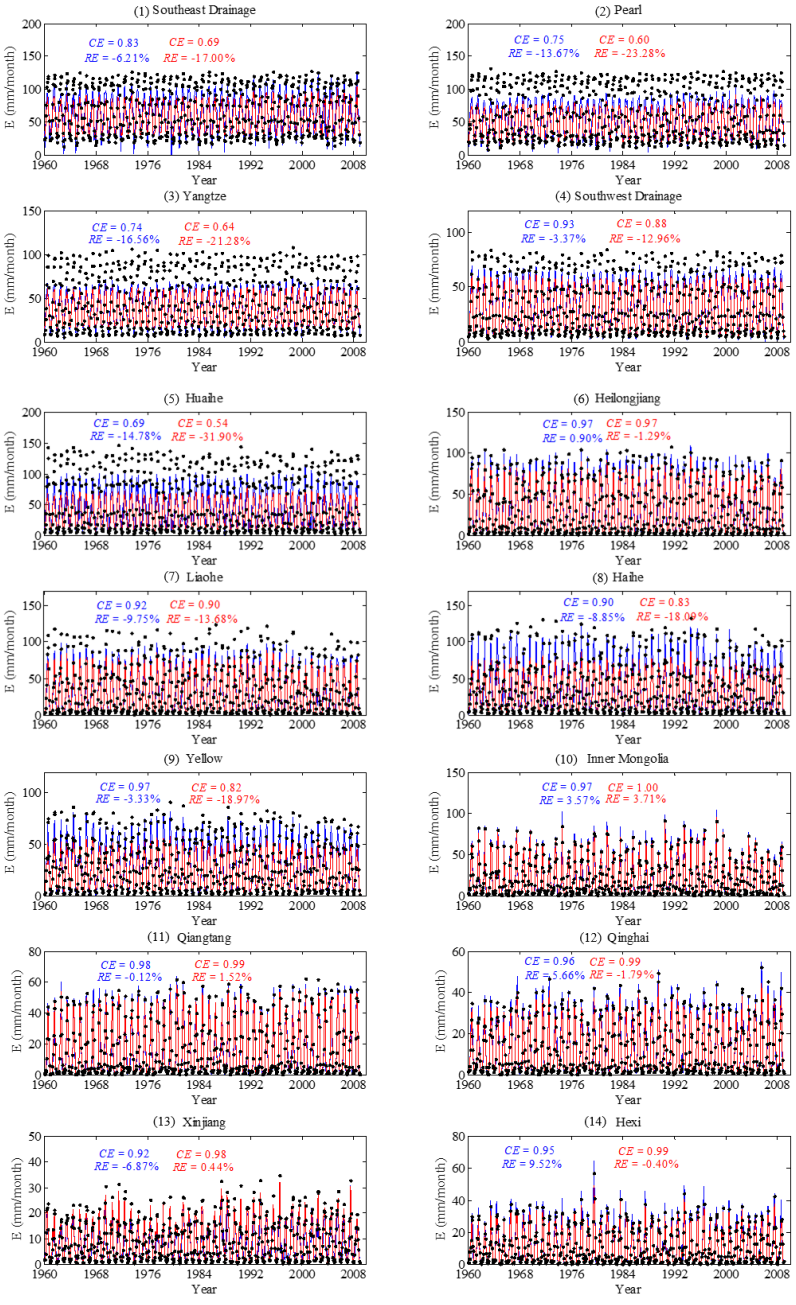

Figure 9. Comparison of monthly time series of observed *E* (black dots) with that predicted by the BM (blue line) and that predicted by the extended BM (red line) for each of the 14 basins. The number in the parentheses is consistent with that given in Table 1.

Hydrol. Earth Syst. Sci. Discuss., https://doi.org/10.5194/hess-2017-441
Manuscript under review for journal Hydrol. Earth Syst. Sci.
Discussion started: 25 August 2017

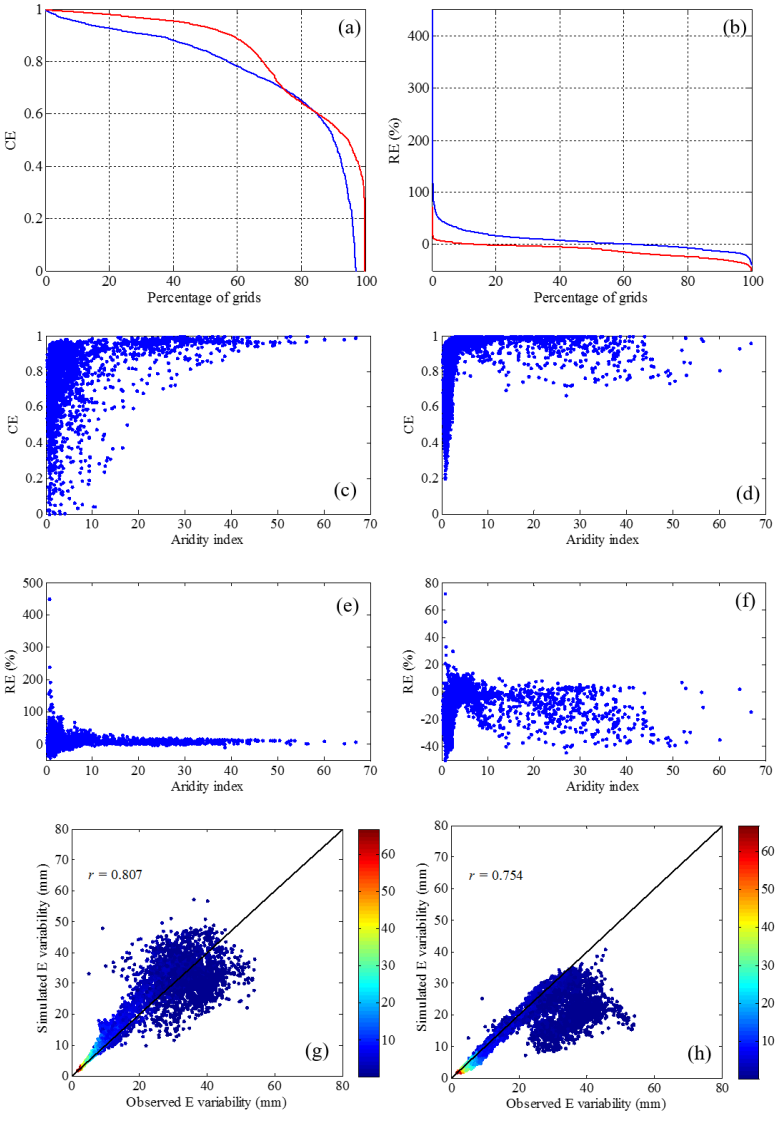

Figure 10. Model validation at the monthly timescale: (a) the cumulative distribution of the percentage of grids with the *CE* larger than or equal to a specific value for the BM (blue line) and the extended BM (red line); (b) same as (a), but for *RE*. The relationship between *CE* and the aridity index for (c) the BM and (d) the extended BM for the total 3814 grids over China. The relationship between *RE* and aridity index for (e) the BM and (f) the extended BM. Comparison of observed and simulated *E* variability for (g) the BM and (h) the extended BM. The color bar indicates the mean annual aridity index for the total 3814 grids over China.

Hydrol. Earth Syst. Sci. Discuss., https://doi.org/10.5194/hess-2017-441
Manuscript under review for journal Hydrol. Earth Syst. Sci.
Discussion started: 25 August 2017

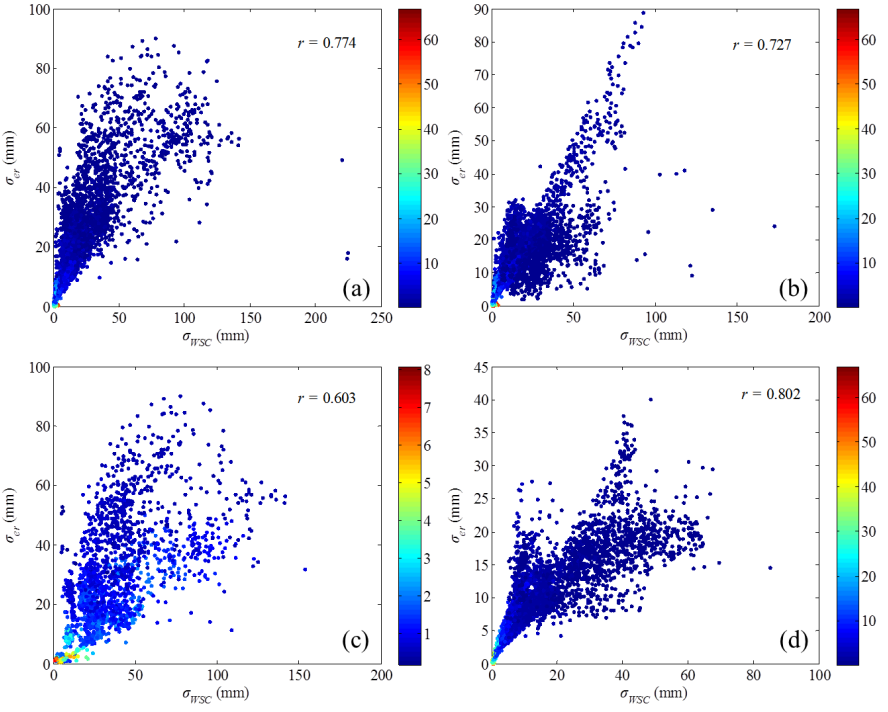

Figure 11. The temporal variability (i.e., standard deviation) of the modeling errors in *E* (i.e., the simulated *E* of the BM minus the observed *E*) versus that of *WSC* at the (a) annual, (b) dry season, (c) wet season, and (d) monthly timescales. The color bar indicates the mean annual aridity index of the selected grids.

Hydrol. Earth Syst. Sci. Discuss., https://doi.org/10.5194/hess-2017-441
Manuscript under review for journal Hydrol. Earth Syst. Sci.
Discussion started: 25 August 2017

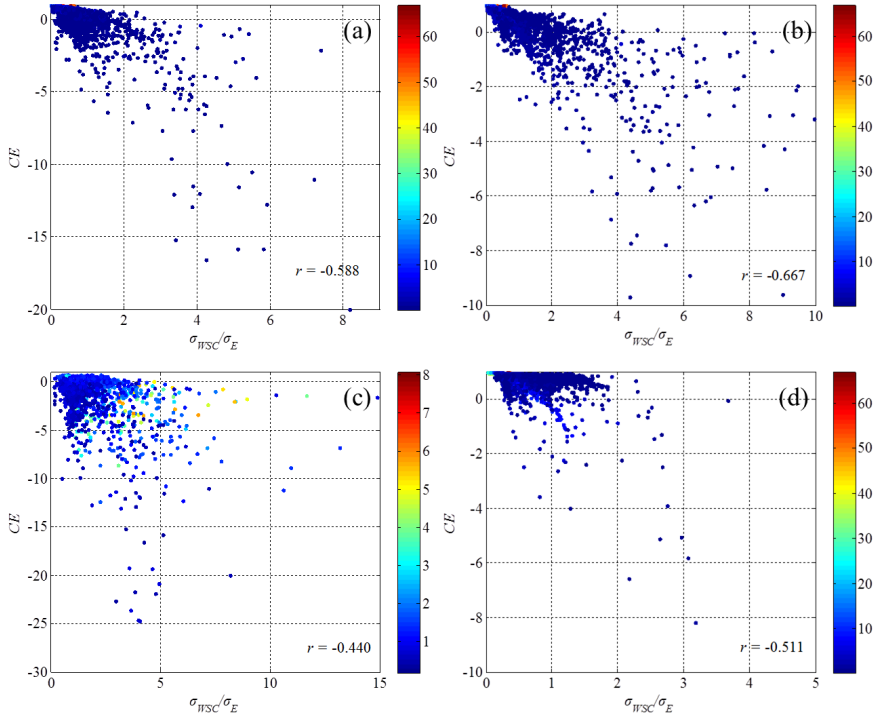

Figure 12. The ratio of the standard deviation of *WSC* to that of *E* versus the *CE* of the BM simulations at the (a) annual, (b) dry season, (c) wet season, and (d) monthly timescales. The color bar indicates the mean annual aridity index of the selected grids.

Hydrol. Earth Syst. Sci. Discuss., https://doi.org/10.5194/hess-2017-441
Manuscript under review for journal Hydrol. Earth Syst. Sci.
Discussion started: 25 August 2017

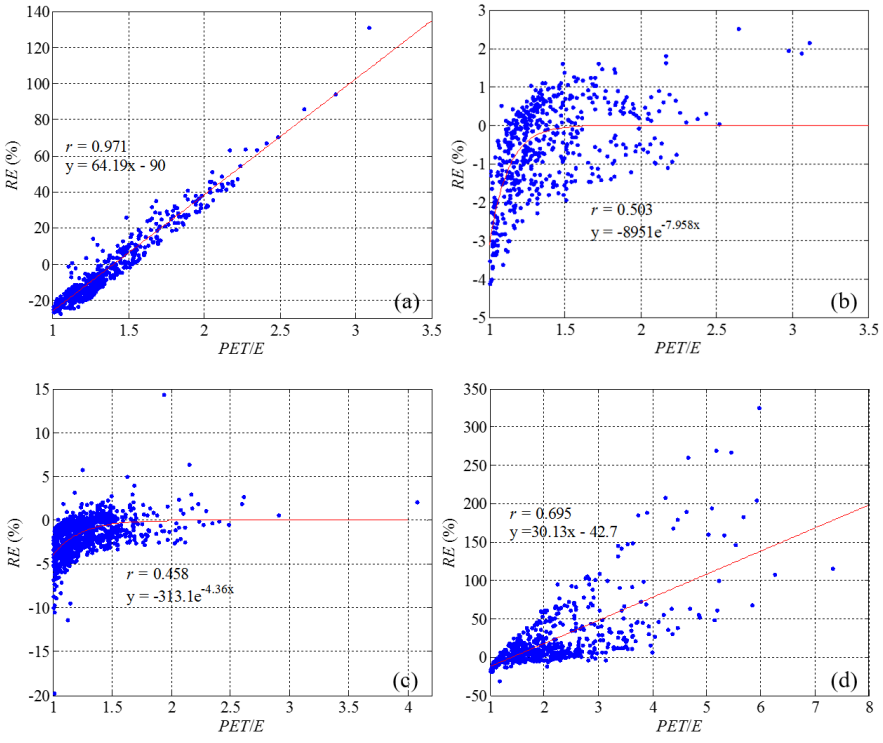

Figure 13. The relationship between the mean *RE* of *E* and the mean ratio of *PET*/*E* for the 622 grids under the energy-limited condition with (a) mean annual, (b) annual, (c) wet seasonal, and (d) monthly timescales.